Nanoscale Res Lett (2007) 2:461–468
DOI 10.1007/s11671-007-9087-z

NANO EXPRESS

Hydrothermal synthesis of amorphous MoS_2 nanofiber bundles via acidification of ammonium heptamolybdate tetrahydrate

G. Nagaraju · C. N. Tharamani · G. T. Chandrappa · J. Livage

Received: 16 March 2007 / Accepted: 10 August 2007 / Published online: 1 September 2007

Abstract MoS_2 nanofiber bundles have been prepared by hydrothermal method using ammonium molybdate with sulfur source in acidic medium and maintained at 180 °C for several hours. The obtained black crystalline products are characterized by powder X-ray diffraction (PXRD), Fourier transform infrared spectrometer (FTIR), X-ray photoelectron spectroscopy (XPS), scanning electron microscopy (SEM) and transmission electron microscopy (TEM). The PXRD pattern of the sample can be readily indexed as hexagonal 2H-MoS_2. FTIR spectrum of the MoS_2 shows the band at 480 cm^{-1} corresponds to the γ_{as}(Mo-S). SEM/TEM images of the samples exhibit that the MoS_2 nanofiber exist in bundles of 120–300 nm in diameter and 20–25 μm in length. The effects of temperature, duration and other experimental parameters on the morphology of the products are investigated.

Keywords Hydrothermal · Nanofiber bundles · MoS_2 · Citric acid

G. Nagaraju · G. T. Chandrappa (✉)
Department of Chemistry, Central College Campus, Bangalore University, Bangalore 560001, India
e-mail: gtchandrappa@yahoo.co.in

C. N. Tharamani
Department of Chemistry, University of Saskatchewan, Saskatoon, Canada SK S7N 5C9

J. Livage
Laboratoire Chimie de la Matière Condensée, Université Pierre et Marie Curie, 4 place Jussieu, Paris cedex 05 75252, France

Introduction

Nowadays, one-dimensional nanostructural materials (nanorods, nanowires, nanobelts and nanotubes) have attracted heightened attention because of their potential applications in nanodevices and functional materials [1]. Continuous effort has been devoted to the investigation on the crystalline phases of the layered transition metal dichalcogenides, because of their unusual crystal structure and unique physical and chemical properties [2]. In analogy to graphite, nanoparticles of many inorganic compounds such as MoS_2, WS_2 are not stable against folding, and can adopt nanotubular and fullerene-like structures [3]. As transition metal sulfides, MoS_2 has been the subject of significant research for applications including nonaqueous lithium batteries, catalytic hydride sulfurization of petroleum and wear resistance. For each of these applications, the important processes occur either at the surface or at the exposed edges of the MoS_2 layers [1]. MoS_2 is a layered semiconductor (band gap = 1.2 eV, indirect) that resists oxidation even in moist air at temperatures up to 85 °C [4]. This attribute makes MoS_2 an attractive semiconductor material for nanoscience applications. Recent studies have suggested that reducing the size of the MoS_2 crystals can improve their lubrication properties in bearings, O-rings or other heavy—wear applications [5].

Inorganic syntheses using organic surfactants are successfully applied for the preparation of various nanostructural materials [6, 7]. The subsequent template elimination without destruction of the mesoporous texture remains a difficult step [8]. Various methods of preparation includes chemical vapor deposition, sol–gel processing, spray pyrolysis, co-precipitation, sonochemical synthesis, metathesis reactions, two step electrochemical synthesis etc are having been in practice [9–12]. Tenne and co-workers

[13, 14] first reported the production of fullerene-like MoS_2 nanotubes via the gas phase reaction between MoO_{3-x} and H_2S in a reducing atmosphere at elevated temperature (800–1000 °C). Rao and co-workers obtained MoS_2 nanotubes by simple heating MoS_3 in a stream of hydrogen under high temperature [15]. Zelenski et al. [16] synthesized fibers and tubules of MoS_2 by the thermal decomposition of ammonium thiomolybdate precursors at 450 °C. MoS_2 nanotubes [17] were made by subliming 2H–MoS_2 powder in presence of H_2S at 1300 °C. Recently MoS_2 nanorods [18] were synthesized using α-MoO_3 nanorods with a mixture of $H_2S \cdot H_2$ (15 vol% of H_2S) for 4 h at several temperatures. However, almost all the methods to obtain MoS_2 nanotubes and nanorods utilize high temperature gas-solid reaction under reducing gas atmosphere. Yumei et al. [1, 19] synthesized MoS_2 nanorods and nanospheres by hydrothermal method using ammonium molybdate with Na_2S in presence of $NH_2OH \cdot HCl$ as oxidizing agent. Hydrothermal synthesis is becoming popular for environmental reason, since water is used as reaction solvent than organics. This method has been widely used to prepare nanostructures due to its simplicity, high efficiency and low cost.

In this article, as a part of our recent efforts on the investigation of 1-D materials [20], we report a simple low temperature hydrothermal method for preparation of MoS_2 nanofiber bundles with morphology control. We examined the effect of precursors (ammonium molybdate, sodium sulphide and citric acid) concentration, duration and the temperature on the morphology of the product. Finally, we discuss appropriate conditions for producing MoS_2 nanobundles.

Experimental section

Synthesis

The hydrothermal process was carried out like our previous report [21, 22] to prepare MoS_2 nanofiber bundles. In a typical synthesis of MoS_2 nanofibers, sodium sulfide and H_2S gas were used as sulfur sources in order to investigate the source effect on the morphology of the product.

In the first trail 1.235 g ammonium heptamolybdate tetrahydrate ($(NH_4)_6Mo_7O_{24} \cdot 4H_2O$) was put into 25 mL distilled water under continuous stirring. After 10 min, 0.5 g citric acid monohydrate ($C_6H_8O_7 \cdot H_2O$) was added to the above solution. To this solution mixture, 0.312 g sodium sulfide crystals were added. The initial greenish black color was changed to red after 1h stirring on a magnetic stirrer. In the subsequent trail, 0.5 g ammonium heptamolybdate tetrahydrate was put into 25 mL distilled water under continuous stirring. H_2S gas is passed in to the warmed acidified with dilute HCl solution for about 5–8 min.

The sealed 25 mL Teflon lined autoclaves containing above solution mixture were placed for hydrothermal treatment at 180 °C for several hours. The autoclaves were cooled and the resulted black solid was retrieved from the solution by centrifugation, washed with distilled water followed by ethanol to remove the ions possibly remaining in the end product, and finally dried in air.

Characterization

Powder X-ray diffraction data were recorded on Philips X'pert PRO X-ray diffractometer with graphite monochromatized Cu Kα radiation ((= 1.541 Å). The Fourier transform infrared spectrum of the samples was collected using Nicollet FTIR spectrometer. Scanning electron micrograph images were taken with JEOL (JSM—840 A) scanning electron microscope. X-ray photoelectron spectroscopy was carried out on an ESCA-3 Mark II X-ray photoelectron spectrometer, (VG Scientific, UK) using Al Kα radiation (1486.6 eV) as the exciting source. The morphology of the samples was observed using (H-800EM Japan Hitachi) transmission electron microscope (TEM) equipped with EDS (Kevex Sigma TM Quasar, USA) to measure the elements contained in the samples.

Results and discussion

Figure 1a, b shows the PXRD patterns of the samples prepared using sodium sulfide and H_2S as sulfur sources in acidic medium at 180 °C for 48 and 24 h, respectively. It shows only a broad, weak envelope beginning at $2\theta = 30°$ and continuing out above 60°, the two maxima approximately located at the *100* and *110* positions of bulk 2H–MoS_2 [23]. The PXRD patterns resemble that of the single-layer MoS_2 prepared by exfoliation method [24]. All the diffractions can be readily indexed as hexagonal 2H–MoS_2 [space group $P6_3/mmc$ (194)] with lattice constants $a = 3.16116$ Å and $c = 12.2985$ Å, identical to the reported data in the JCPDS cards (37–1492). At 180 °C only poor crystals were produced. The absence of the *002* diffraction at $2\theta = 14.4°$ suggests that absence of stacking, thus the sample should be an aggregate of single sheets of MoS_2 [1, 8, 18, 23, 25].

Chemical analysis using EDS indicates the presence of Mo and S (elements of MoS_2), and no other elements existed as observed in Fig. 2. Furthermore, the quantification of the peaks shows that the atomic ratio of S to Mo is 1.92, which is very close to the stoichiometric MoS_2. From the IR spectrum (Fig. 3), it is observed that the band at 480 cm^{-1} corresponds to γ_{as}(Mo–S). The bands above 600 cm^{-1} correspond to Mo–O vibrations and they indicate

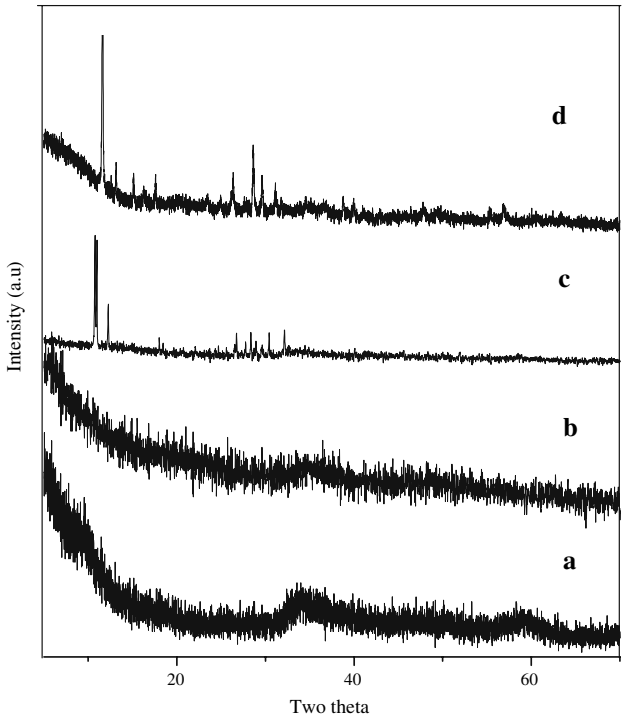

Fig. 1 Powder XRD pattern of MoS_2 nanofiber bundles prepared at (**a**) 180 °C for 48 h using Na_2S as sulfur source with 0.5 g citric acid. (**b**) 180 °C for 24 h using H_2S as sulfur source. (**c**) 180 °C for 48 h using Na_2S as sulfur source without citric acid. (**d**) 180 °C for 48 h using Na_2S as sulfur source with 1 g citric acid

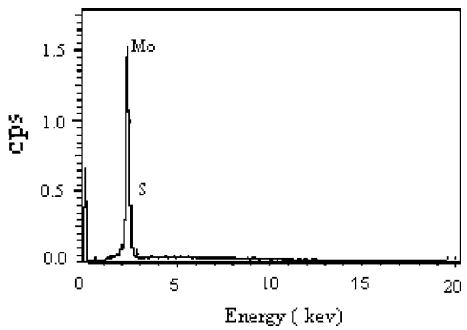

Fig. 2 EDS pattern of MoS_2 nanofiber bundles prepared at 180 °C for 48 h

that oxygen is present in similar types of coordination as in MoO_3. We assign the band at 941 cm^{-1} to the γ_{as}(Mo–O) vibrations of terminal (–Mo=O) group and 693 cm^{-1} to γ(Mo–O) vibrations. The frequency of the vibration is shifted to the lower wavenumber compare to its standard value in crystalline MoO_3, due to the presence of reduced Mo centers and sulfur as a ligand [26].

X-ray photoelectron spectra of Mo(3d) and S(2p) core level regions of as-prepared nanoparticles are shown in Fig. 4a and b and the values are tabulated in Table 1. Mo(3d) peaks in as-prepared nanoparticles were deconvoluted into

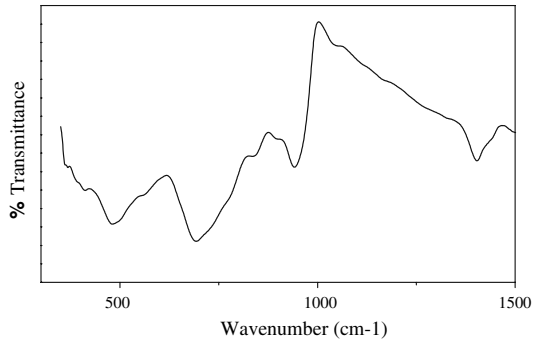

Fig. 3 FTIR spectrum of MoS_2 nanofiber bundles prepared at 180 °C for 48 h

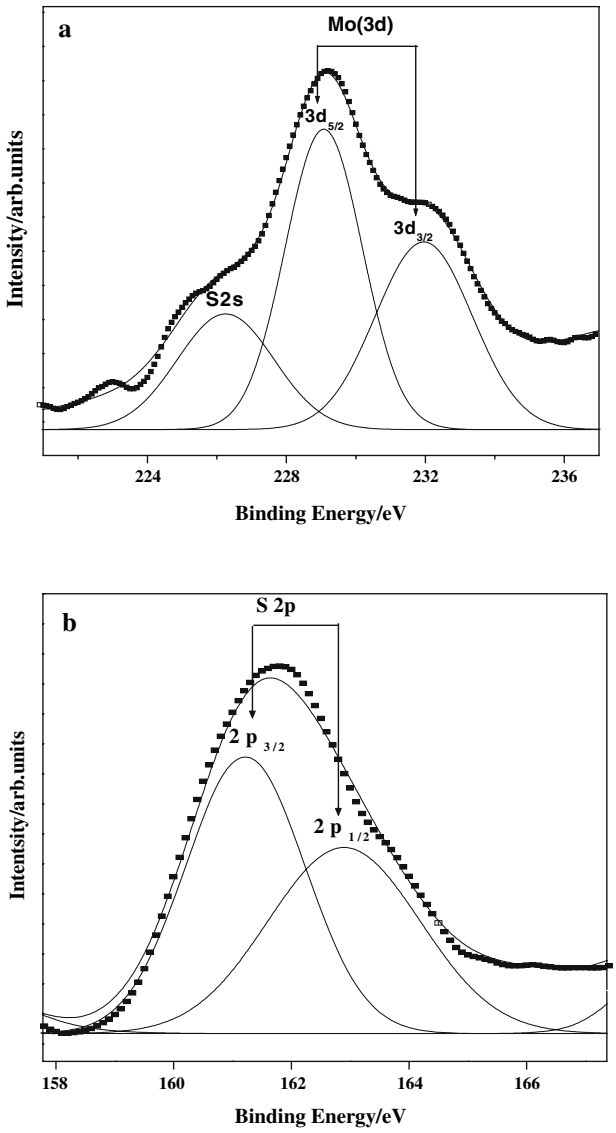

Fig. 4 XPS pattern of MoS_2 nanofiber bundles prepared at 180 °C for 48 h

Table 1 XPS data of Mo(3d) and S(2p)

Peak	Area	Binding energy (eV)	FWHM (eV)	Peak height (Intensity)
$Mo3d_{3/2}$	481.32	232.1	2.7661	138.84
$Mo3d_{5/2}$	612.97	229.1	2.1874	223.59
S2s	295.81	226.25	2.7571	85.605
$S(2p_{3/2})$	113.89	161.25	2.0538	44.248
$S(2p_{1/2})$	110.89	162.94	2.8032	31.562

WHM = Full Width Half Maximum

sets of spin-orbit doublet. Accordingly, the high intense $Mo(3d_{5/2})$ peaks at 229.1 and low intense $Mo(3d_{3/2})$ peak at 232.1 eV could be attributed to MoS_2. Whereas lower binding energy shoulder peak at 226.25 eV is because of S(2s) [27].

Figure 4b shows S(2p) doublet peak ($2p_{3/2}$ and $2p_{1/2}$) at 161.25 and 162.94 eV respectively in which $2p_{3/2}$ and $2p_{1/2}$ orbital peaks coincide with each other. It is to be noted that the peak positions of S(2p) and $Mo(3d_{5/2})$ for MoS_2 is in good agreement with he results on MoS_2 [28].

The chemical shifts of $Mo(3d_{5/2})$ and S(2p) in MoS_2 nanoparticle is +1.6 and –2.2 eV in comparison to elemental Mo and S [29]. The electronegativity of S being 2.5 is greater than that of Mo being 1.8. Therefore there occurs some partial electron transfer from molybdenum to sulfur. As a result, molybdenum becomes positively charged as shown by the increase in binding energy and sulfur becomes negatively charged as shown by the decrease in binding energy.

MoS_2 nanofiber of about 120–300 nm in diameter and 20–25 μm in length are identified from SEM images (Fig. 5). They are well aligned and occur in-group of bundles with very high aspect ratio. It can be seen that the nanofiber self assembled into bundles and the nanofiber in a bundles had the same growth direction. The morphology and structure of individual MoS_2 nanorods have been characterized in further detail using TEM, which are shown in Fig. 6. It can be seen that the nanorods are straight and uniform along their entire length and thickness of about up to 300 nm. The ends of the nanorods are broken. Figure 6d is the high resolution TEM image of the MoS_2 nanorods and this image shows solid nanorods are uniform in thickness.

The reduction of transition metal ions by surfactant is useful for the production of ultra fine particles of metal sulfides. Unfortunately, molybdic compound reduction chemistry is quite complex and the nature of the products strongly depends on the reaction conditions. For example, Afanasiev et al. show that the reduction of aqueous ammonium molybdate at different temperatures and conditions yields binary sulfides such as $MoS_{5.6}$, MoS_6, and MoS_3 as well as binary oxides such as MoO_3 and MoO_2. In fact, the mechanism differs markedly in aqueous and in nonaqueous solutions. In order to disclose the transition

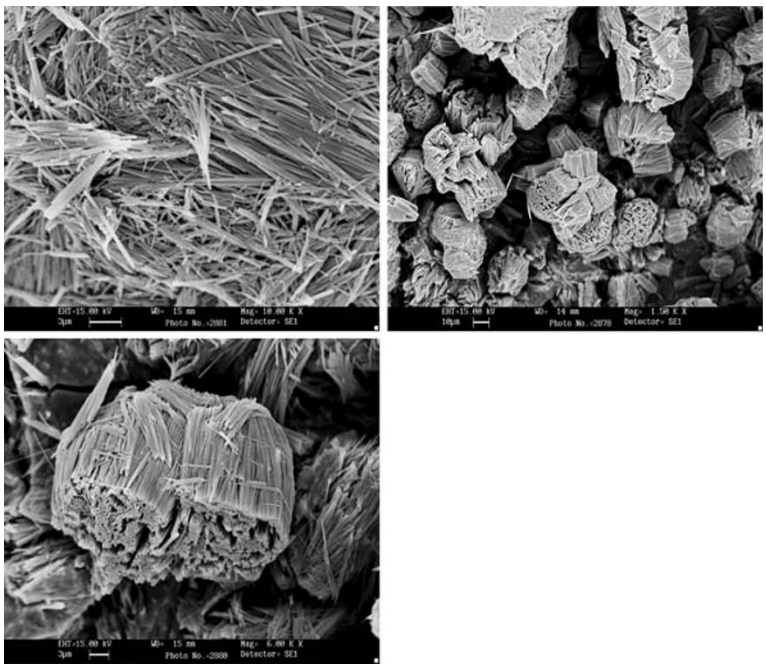

Fig. 5 SEM images of MoS_2 nanofiber bundles prepared at 180 °C for 48 h

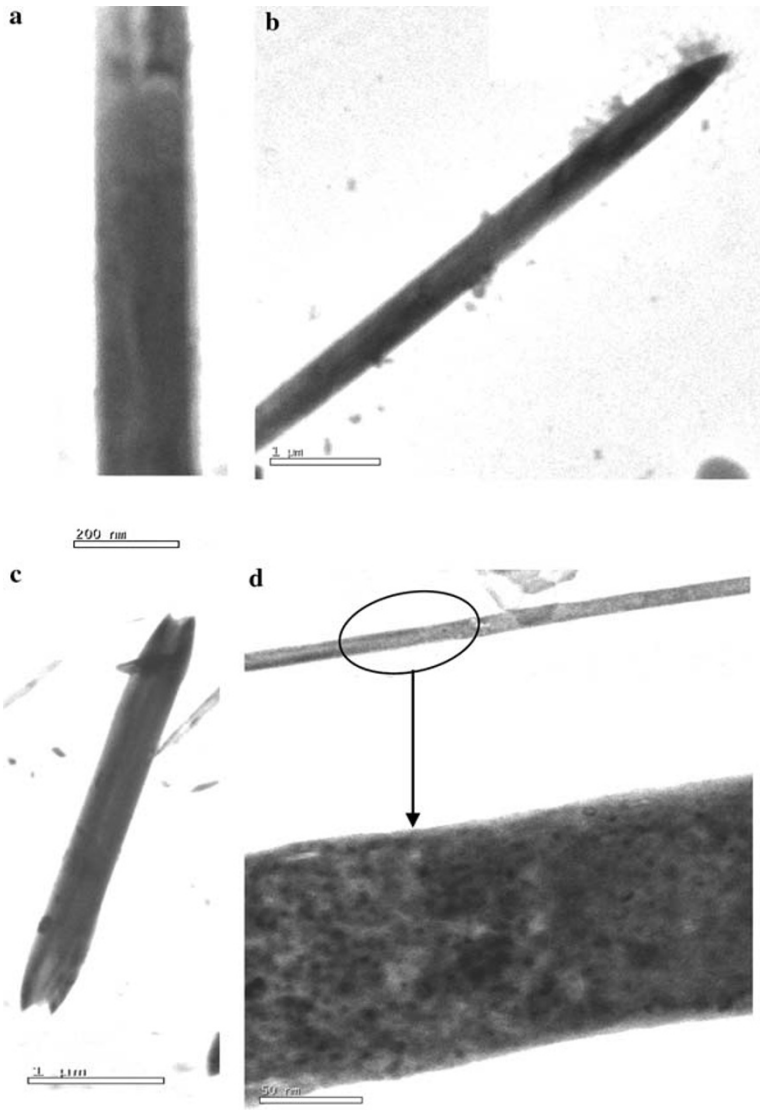

Fig. 6 TEM images of MoS_2 nanofiber bundles prepared at 180 °C for 48 h

process from $(NH_4)_6Mo_7O_{24} \cdot 4H_2O$ to MoS_2, the role of citric acid [30–32] on phase of products was investigated. The possible reaction mechanism can be written as

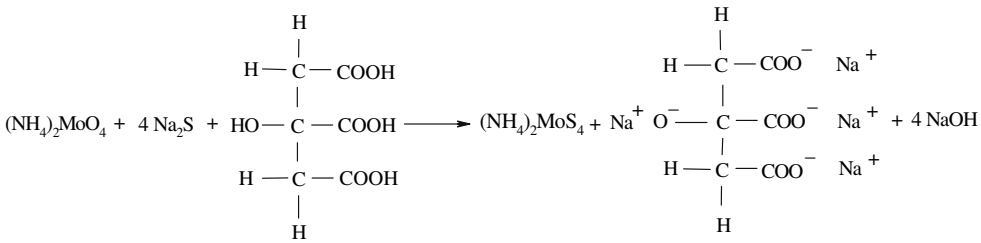

(1)

reduction reaction under hydrothermal conditions. Thus by the addition of 1 g of citric acid or without citric acid, sulfureted reaction and reduction reaction do not react completely so that the products consist of much MoO_3 phase as shown in the Fig. 1c, d. Therefore during the formation of MoS_2 nanofiber bundles, citric acid plays a very prominent role. Figure 7a, b gives the SEM images of

$$(NH_4)_2MoS_4 \rightarrow MoS_2 + N_2 + 2H_2 + 2H_2S \quad (2)$$

Step 1 is a sulfureted reaction, in which an intermediate phase $(NH_4)_2MoS_4$ is produced [33], and step 2 is a

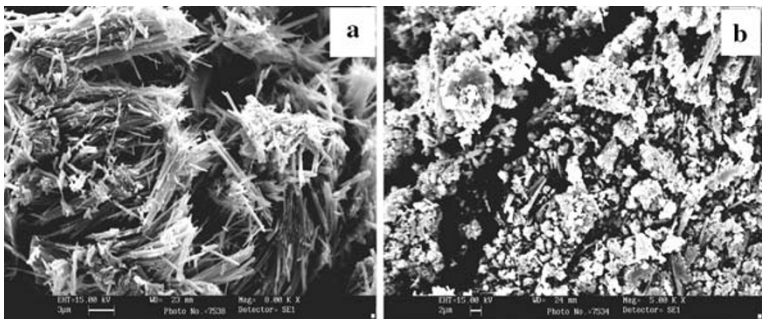

Fig. 7 SEM images of MoS_2 nanofiber bundles prepared at (**a**) 180 °C for 48 h with 1 g citric acid and (**b**) without citric acid

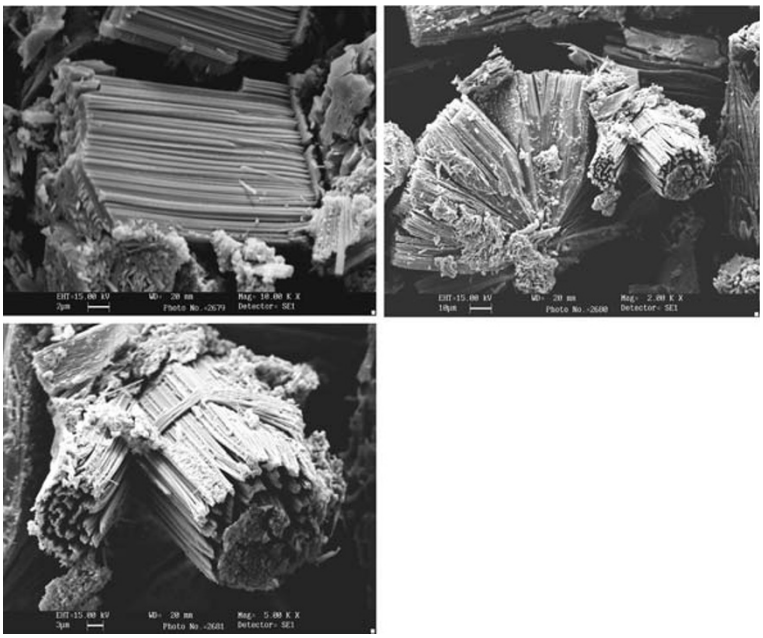

Fig. 8 SEM images of MoS_2 nanofiber bundles prepared at 180 °C for 24 h using H_2S as sulfur source

the product prepared with and without citric acid. We evaluate the effect of temperature and duration on the morphology of the products. But there was no interesting morphology of the product obtained.

The morphology of the product prepared at 180 °C for 24 h (Fig. 8) using H_2S resembles with the morphology of the product prepared at 180 °C for 48 h (Fig. 5) using sodium sulfide as sulfur source. Here, there is a regular arrangement of MoS_2 fibers takes place to form bundles. The thickness of the fiber is found to be about 300 nm and length is about 12 μm. From the SEM images, we observed that the length of all fibers is found to be same with sharp ends having voids in each MoS_2 bundles.

The possible reaction mechanism can be written when H_2S as sulfur source is

$$(NH_4)_2MoO_4 + 6HCl \rightarrow MoCl_4 + 4H_2O + 2\,NH_3 + Cl_2 \quad (3)$$

$$MoCl_4 + 2\,H_2S \rightarrow MoS_2 + 4\,HCl \quad (4)$$

Step 3 is a reduction reaction, in which an intermediate phase $MoCl_4$ is produced [19], and step 4 is a sulfureted reaction under hydrothermal conditions.

Figure 9a, b shows the SEM images of MoS_2 prepared at 180 °C for 16 and 20 h. When the duration is increased to 48 h, nanorods (Fig. 9c) are obtained. The thickness of the nanorods is found to be in the range of 200–600 nm.

Conclusion

Nanofiber of MoS_2 bundles with 150–300 nm in diameters and 20–25 μm in length have been successfully synthesized by a simple low temperature hydrothermal method. PXRD pattern indicated the amorphous MoS_2 was made up of single layer and layer stacking had not taken place. The

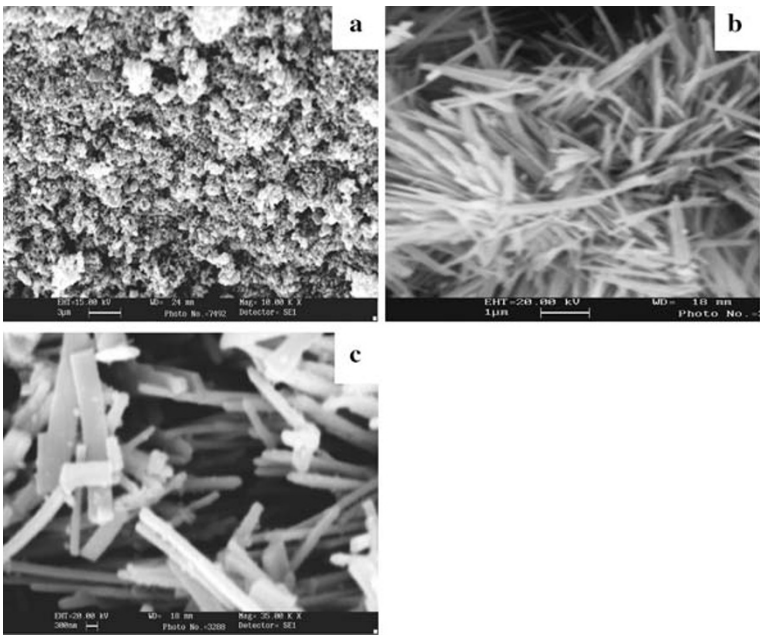

Fig. 9 SEM images of MoS_2 nanofiber bundles prepared at 180 °C h using H_2S for (**a**) 16 h (**b**) 20 h and (**c**) 48 h

nanofiber self assembled into bundles and the nanofiber bundle had the same growth direction. SEM study reveals the formation of bundles of well-aligned MoS_2 nanofiber with very high aspect ratio. Since the MoS_2 nanomaterials are often very difficult to prepare and the search for more simple routine is quite valuable with regard to energy-saving and less pollution. It can be demonstrated that the optimum conditions for preparing MoS_2 nanofiber are at 180 °C for 48 h using citric acid and 180 °C for 24 h by passing H_2S in presence of HCl. Under these conditions the morphology of the products resembles to one another.

Acknowledgments The author G. T. Chandrappa thankful to the Department of Science and Technology, NSTI Phase-II, New Delhi, Government of India for financial support to carryout this research work. We also thank the Central Facility, Dept. of Physics and Dept. of Metallurgy, Indian Institute of Science, Bangalore for collecting XRD data and SEM images.

References

1. Y. Tian, J. Zhao, W. Fu, Y. Liu, Y. Zhu, Z. Wang, Mater. Lett. **59**, 3452 (2005)
2. J.A. Wilson, F.J. Di Saluo, S. Majaham, Adv. Phys. **24**, 117 (1972)
3. C.N.R. Rao, Manish Nath. Dalton Tran. 1 (2003)
4. S. Ross, A. Sussman, J. Phys. Chem. **59**, 889 (1995)
5. C.L. Stender, E.C. Greyson, Y. Babayan, T.W. Odom, Adv. Mater. **17**, 2837 (2005)
6. F. Krumeich, H.J. Muhr, M. Neiderberger, F. Bieri, B. Schnder, R. Nesper, J. Am. Chem. Soc. **121**, 8324 (1999)
7. O. Durupthy, M. Jaber, N. Steunou, J. Maquet, G.T. Chandrappa, J. Livage, Chem. Mater. **17**, 6395 (2005)
8. P. Afanasiev, G.-F. Xia, G. Berhault, B. Jouguet, M. Lacroix, Chem. Mater. **11**, 3216 (1999)
9. M.R. Close, J.L. Petersen, E.L. Kugler, Inorg. Chem. **38**, 1535 (1999)
10. M.M. Mdleleni, T. Hyeon, K.S. Suslick, J. Am. Chem. Soc. **120**, 6189 (1998)
11. P.R. Bonneau, R.F. Jarvis Jr., R.B. Kaner, Nature **349**, 510 (1991)
12. Q. Li, J.T. Newberg, E.C. Walter, J.C. Hemminger, R.M. Penner, Nano Lett. **4**, 277 (2004)
13. R. Tenne, L. Margulus, M. Genut, G. Hodes, Nature **36**, 444 (1992)
14. Y. Feldman, G.L. Frey, M. Homyonfer, V. Lyakhovitskaya, L. Margulis, H. Cohen, G. Hodes, J.L. Hutchison, R. Tenne, J. Am Chem. Soc. **118**, 5362 (1996)
15. M. Nath, A. Govindaraju, C.N.R. Rao, Adv. Mater. **13**, 283 (2001)
16. C.M. Zelenski, P.K. Dorhout, J. Am. Chem. Soc. **120**, 734 (1998)
17. W.K. Hsu, B.H. Chang, Y.Q. Zhu, W.Q. Han, H.M. Terrones, N. Grobert, A.K. Cheetham, H.W. Kroto, D.R.M. Walton, J. Am. Chem. Soc. **122**, 10155 (2000)
18. M.A. Albiter, R. Huirache-Acuna, F. Paraguay-Delgado, J.L. Rico, G. Alonso-Nunez, Nanotechnology **17**, 3473 (2006)
19. Y. Tian, X. Zhao, L. Shen, F. Meng, L. Tang, Y. Deng, Z. Wang, Mater. Lett. **60**, 527 (2006)
20. B. Nagappa, G.T. Chandrappa, Jacques Livage, Pramana-J. Phys. **65**, 917 (2005)
21. G.T. Chandrappa, N. Steunou, S. Cassaignon, C. Bisvais, P.K. Biswas, J. Livage, J. Sol-Gel Sci. Tech. **26**, 593 (2003)
22. G.T. Chandrappa, J. Livage, Syn. React. Inorg. Met.-Org. Nano-Met. Chem. **36**, 23 (2006)
23. P. Joensen, R.F. Frindt, S.R. Morrison, Mater. Res. Bull. **21**, 457 (1986)
24. Y. Peng, Z. Meng, C. Zhong, J. Lu, W. Yu, Z. Yang, Y. Qian, J. Solid State Chem. **159**, 170 (2001)
25. Y. Tian, Y. He, Y. Zhu, Mater. Chem. Phys. **87**, 87 (2004)
26. Th. Weber, J.C. Muijsers, J.H.M.C. Van Wolput, C.P.J. Verhagen, J.W. Niemantsverdriet, J. Phys. Chem. **100**, 14144 (1996)
27. D. Briggs, M.P. Seah, *Practical Surface Analysis by Auger and X-ray Photoelectron Spectroscopy* (Wiley New York 1984), p. 503
28. J. Pouzet, H. Hadouda, J.C. Bernede, R. Le Ny, Phys. Chem. Solids **57**, 1363 (1996)

29. W. Wang, P. Skeldon, G.E. Thompson, Surf. Coat. Technol. **91**, 200 (1997)
30. M. Matzapetakis, C.P. Raptopolou, A. Tsohos, V. Papaefthymiou, N. Moon, A. Salifoglou, J. Am. Chem. Soc. **120**, 13266 (1998)
31. J.-d. Tsay, T.-t. Fang, J. Am. Ceram. Soc. **82**, 1409 (1999)
32. M. Kakihana, T. Nagumo, M. Okamoto, H. Kakihana, J. Phys. Chem. **91**, 6128 (1987)
33. W. Pan, M.E. Leonowicz, E.I. Stiefel, Inorg. Chem. **22**, 612 (1983)